

Chemical and Solar Electric Propulsion Systems Analyses for Mars Sample Return Missions

Benjamin B. Donahue[†]

Boeing Phantom Works, Huntsville, AL 35806

Shaun E. Green*

Science Applications International Corporation, Huntsville, AL 35806

Victoria L. Coverstone[§], Byoungsam Woo^δ

University of Illinois at Urbana-Champaign, Urbana, IL 61801

Conceptual in-space transfer stages, including those utilizing solar electric propulsion, chemical propulsion, and chemical propulsion with aerobraking or aerocapture assist at Mars, were evaluated. Roundtrip Mars sample return mission vehicles were analyzed to determine how specific system technology selections influence payload delivery capability. Results show how specific engine, thruster, propellant, capture mode, trip time and launch vehicle technology choices would contribute to increasing payload or decreasing the size of the required launch vehicles. Heliocentric low-thrust trajectory analyses for Solar Electric Transfer were generated with the SEPTOP code.

		Nomenclature	
ACS	= Attitude control system	LV	= Launch vehicle
AU	= Astronautical unit	MSR	= Mars sample return
C3	= Trajectory energy (V_{hp}^2)	Po	= Solar array power
dV	= Delta-velocity	PPU	= Power processing unit
IPS	= Ion Propulsion system	RCS	= Reaction control system
Isp	= Impulse specific	T/W	= Thrust-to-weight ratio
LMO	= Low Mars orbit	Vhp	= Hyperbolic velocity

I. Introduction

Mars Sample Return (MSR) mission in-space transfer craft capable of delivering payloads to, and returning payloads from, Mars over the years 2009-2018 were investigated. Results show how propulsion system, propellant, staging, trajectory, trip time and launch vehicle choices affect delivered payload capabilities. Chemical propulsion MSR spacecraft, utilizing five different propellant combinations (Nitrogen Tetraoxide (NTO)/ Hydrazine (N_2H_4), Liquid Oxygen (O_2/N_2H_4), O_2 /Methane (CH_4), Fluorine (F_2)/ N_2H_4 and O_2 /Hydrogen (H_2)) were compared to Solar Electric Propulsion (SEP) MSR spacecraft utilizing Xenon ion and Hall thrusters. The MSR transfer stage captures at Mars either propulsively or aerodynamically; the Mars lander separates previous to the capture burn or after insertion with the transfer stage into a 400 km circular Low Mars Orbit (LMO). In LMO the transfer stage waits until the next minimum-energy return opportunity. Before departure, the MSR transfer stage rendezvous with the sample carrying Mars ascent stage, retrieves the sample payload canister and departs for Earth. At Earth arrival, the sample payload, in a reentry capsule, returns via direct entry and the transfer stage is expended. For the SEP analyses, the SEP Trajectory Optimization Program (SEPTOP) was used. The SEP trajectory optimization process includes launch vehicle injected mass capability as a function of C3 as an optimization constraint; conversely, C3 was held to a fixed value for the high thrust chemical vehicles. Mars lander payload is either set to a reference value of 1.2 mt or is a variable to be optimized consistent with constraints, such as launch vehicle capability. In all cases, a 0.15 mt sample module is collected in LMO and returned to Earth. Subsequent to the generation of the results, vehicle system modeling tools were further refined, and the results presented here, generated in 2003, do not reflect the latest modeling improvements. Updated results may be presented at a later date.

[†] Third Generation Space Technology Lead, Transformational Space Systems, 950 Explorer Blvd, MC JV-03, AIAA Associate Fellow

* Systems Engineer, Engineering and Technology Section, 6725 Odyssey Discovery Dr., AIAA Associate Fellow

§ Associate Professor, Department of Aerospace Engineering, 306 Talbot Lab, MC 236, AIAA Associate Fellow

δ Graduate student, Department of Aerospace Engineering, 327 Talbot Lab, MC 236

II. Solar Electric Propulsion Vehicle Modeling

For purposes of generating optimal low thrust trajectories for the SEP concepts, SEPTOP^{1,2} was used. The trajectory optimization process includes launch vehicle injected mass capability as a function of C3 as an optimization constraint. SEPTOP was utilized to generate the interplanetary trajectories for a variety of relevant launch dates, trip times, departure C3's, arrival velocities, power levels and thruster combinations. The SEPTOP trajectory optimization tool uses launch vehicle performance data to determine the amount of delivered payload mass to the optimal C3 for the particular combination of transfer time, power, and propulsion models. SEP vehicle propellant load, dV, thruster operation time, and thruster throttling and sequencing data are generated as well. Specific thruster models are imbedded into the propulsion system modeling, thereby allowing the investigation of detailed issues such as the effect of available array power on the thrust magnitude and thruster efficiency. Constraints can be placed on major system elements such as the maximum power output from the solar arrays through feathering and the maximum and minimum thruster operational power levels. For all cases a redundant thruster, Power Processing Unit (PPU), propellant management string (PMS) and Digital Control Interface Unit (DCIU) was carried.

III. Chemical Propulsion Vehicle Modeling

For the high thrust chemical propulsion transfer stages, published trajectory data was utilized³. Fixed values for Earth departure C3, Mars arrival hyperbolic velocity (V_{hp}) and Mars departure C3 were used; as were midcourse correction and Earth divert maneuver values. Mars capture and departure chemical propulsion system models consist of experience-based data in the form of curve-fits of historical data and physics-based models. For example, the composite overwrap tank model is scaled from the Advanced X-ray Astrophysics Facility (AXAF) vehicle's composite tank. The baseline chemical capture stage consists of 3 main pressure-fed engines of nominally 100 psia chamber pressure. Main engines are sized for a thrust corresponding to an initial vehicle acceleration of 0.5 at the onset of Mars capture thrusting. Other elements include the Thrust Vector Control (TVC) system, thermal conditioning, pressurization system, and the reaction control systems (RCS). Light weight tanks are operated with tank pressures on the order of 250 psia. Thermal conditioning is assumed to be supplied to tanks, lines, valves and thrusters. The pressurization system consists of high pressure, regulated gaseous He with redundant propellant management system controllers. RCS consists of 16 thrusters, utilizing hydrazine monopropellant at 220 sec Isp.

IV. Assumptions

The propulsion system for each of the chemical stages was configured with the following assumptions:

- 3 main engines, pressure fed; thrust sized for vehicle initial Mars capture of $T/W = 0.5$
- Tankage: pressure feed 250 psia, ullage = 3%
- Engine chamber pressure: 100 psia
- Isp values for the five propellant combinations considered (NTO/N₂H₄, O₂/N₂H₄, O₂/CH₄, F₂/N₂H₄ and O₂/H₂) are 330, 343, 344, 380, and 420 sec respectively.
- Thrust vector control system
- Tank pressurization: high pressure gaseous Helium bottle, regulated

General chemical stage contingencies utilized the following:

- Propellant: 3.0% of total deterministic propellant
- Dry mass: 30% of total mass (non payload) delivered
- Power: provided by batteries
- Structure mass is based on historical data for actual planetary spacecraft
- 2.0% gravity loss penalty for propulsive burns

Reaction Control System (RCS) for the chemical propulsion vehicles followed these assumptions:

- RCS: 16 thrusters, hydrazine monopropellant at 220 sec Isp
- 20 m/s RCS delta-velocity (dV) at Mars includes maintaining final parking orbit
- 10 m/s RCS dV for 3 other events (E & M departure, E arrival)
- 30 m/s dV for course correction and aimpoint maneuvers (each leg)
- 40 m/s dV for the transfer stage Earth divert maneuver at Earth return

Aerocapture assumptions for Mars capture of the chemical vehicles are as follows:

- Initial aerocapture brake mass set to 20% of total captured mass including aeroshell

- Values of 10, 15, 25, and 30% were also evaluated
- A 50 m/s propulsive ΔV applied post aerocapture for periapsis raise maneuver and corrections
- A 85 m/s propulsive ΔV applied for circularization maneuver
- Two capture modes evaluated: Lander Direct Entry (LDE) and Lander captured with orbiter

SEP MSR stages were configured with the following contingencies:

- LV: 2% of launch vehicle nominal capacity baseline (10% also investigated)
- Propellant: 10% of total deterministic Xe propellant
- Dry mass: 30% of dry mass, except 5% on thruster mass
- Power: 5% of baseline array added

SEP MSR stage redundancies and assumptions information:

- 15% reduction in PPU radiator radiant intensity due to view onto solar array
- One extra ion system (thruster, PPU, PMS and DCIU)
- Propulsion system duty cycle = 95% baseline
- Attitude control system (ACS) is provided by Ion Propulsion System (IPS) during low thrust burn.
- ACS is provided by RCS for periods when IPS is not active (coast periods)

SEP MSR power and propulsion system assumptions

- Ion thrusters: NEXT design; Molybdenum grids,
- NEXT performance: 4116 sec Isp, power: 6.85 kWatt (W), thrust: 0.24 N.
- Hall effect thrusters: NASA-173 version 2 design
- Hall performance: 3390 sec Isp, power: 9.95 kW, thrust: 0.36 N
- PPU: NEXT design; state-of-the-art (SOA) heat pipe radiators.
- Xenon tank mass fraction 5%; ullage volume fraction 5%
- Supercritical Xenon propellant: density 3000 kg/m³, temp: 294 deg K, pressure: 34.5 MPa (5000 psia).
- Photovoltaic cells: 23% efficiency
- 2% of array area added per year of propulsion power-on-time for end-of-life requirements
- 10 percent power margin for array
- 250 We spacecraft housekeeping power level
- Spacecraft bus, structures and mechanisms mass based on historical data for actual spacecraft

Launch Vehicle assumptions:

- All launch vehicle payload values used in this analysis contained a 2% margin.
- For chemical MSR missions, launch vehicle provides Earth departure energies of $C3=10 \text{ km}^2/\text{s}^2$
- For SEP MSR missions, launch vehicle $C3$ is variable, though for results presented here, $C3>zero$.

V. Mission and Trajectory Design

In the following sections, mission and trajectory elements will be expounded in sequence with the figures 1-7 in the order of their presentation. Data and information contained in these figures represent a small subset of the total data that was generated for the MSR ISTA study.

SEP CONFIGURATION

A conceptual Earth-Mars-Earth SEP transfer stage is illustrated in Fig. 1, 13, 14 and 15. The vehicle pictured features AEC-Able UltraFlex solar arrays, a spacecraft bus with the necessary avionic, thermal, propellant management and other necessary subsystems and the IPS (Xenon ion thrusters, PPU's and DCIU). An internal Xenon propellant tank is shown inside the bus structure. An aeroentry shell which houses a lander payload is shown with its adapter structure. Ion thrusters provide attitude control (pitch, yaw and roll) during thrusting periods; during coast periods a separate RCS provides control.

LAUNCH VEHICLES

Medium class launch vehicles and their capabilities are listed in Fig. 2. Launcher payload capabilities to $C3$'s of zero and $10 \text{ km}^2/\text{s}^2$ are shown for each launcher with associated margins. These values became the initial mass (M_0) of the combined MSR stage with its Mars payload.

MARS MISSION TRAJECTORY OPTIONS

Possible Mars trajectory selections and options open to the mission designer are listed in Fig. 3. In this analysis, only results for Earth departures $C3$'s of greater than zero are presented. Other selections include conjunction class only trajectories, and return via direct Earth intercept.

EARTH DEPARTURE REQUIREMENTS

High thrust Earth departure $C3$ vs. launch year for the years 2009 through 2024 are shown in Fig. 4. In analyses presented here, all chemical transfer stages featured a fixed launch injection to $C3=10$ (km^2/s^2). $C3=10$ departures cover all but the two most difficult opportunities (2020 and 2022) during this period, as can be seen in Fig. 4. Fixed Mars Vhp values of 3.0 km/s were used, as were Mars departure $C3=3.1$ km^2/s^2 ; these values are typical for 2009-2024 missions³ and were chosen to cover these opportunities.

CHEMICAL MSR ROUNDTRIP DELTA-VELOCITIES

Round trip transfer dV requirements are listed in Fig. 5 for 3 categories corresponding to Mars capture mode:

- all-propulsive capture to LMO
- initial propulsive capture (into a High Mars Orbit (HMO)) followed by aerobraking into LMO
- full aerocapture, followed by a burn to raise periapsis to enter LMO

LMO in all cases is 400 km circular. The total roundtrip dV budget for the aerobraking and aerocapture cases, as a percentage of the all-propulsive case, are 78% and 55%, respectively. A gravity-loss of 2% of the deterministic dV was added in each case. The rendezvous included a 100 m/s dV maneuver to close with the ascent stage sample payload module in LMO.

MARS AEROCAPTURE PARAMETERS

A Mars capture path in which aerocapture is used to decelerate to Mars orbital velocity is shown in Fig. 6. For the MSR cases reported here, the vehicle atmospheric entry interface was set to 120 km altitude; at this point the vehicle begins bank angle modulation for steering to remain within the prescribed flight corridor. Mars closest approach occurs at an altitude of 40 km, the periapsis of the aeropass ellipse; once out of the atmosphere and at apoapsis, a periapsis raise maneuver and correction burn of 50 m/s is applied. Later, an 85 m/s circularization burn completes the transition to the final 400 km circular LMO. Aerocapture provides a 1,160 m/s velocity reduction before exiting the atmosphere. A notional aerocapture maneuver is depicted in Fig. 7.

VI. MSR Transfer Stage Design

In the following section, vehicle and technology elements will be presented in sequence with the figures 8-15.

SEP SOLAR ARRAY INFORMATION

Large, high efficiency solar photovoltaic arrays provide propulsion power and vehicle housekeeping power (with the exception of battery power that must be provided for array deployment). An articulation of the arrays, in one axis relative to the sun, provides array feathering to control array temperature and prevents the solar flux from exceeding a maximum allowable value on the arrays. Able Engineering, a solar array manufacturer, provided Ultra-Flex array modeling characteristics. The Ultra-Flex model represents the present state-of-the-art in lightweight solar array technology. A typical array element is shown in Fig. 8; two of these are shown deployed on Figure 1. Solar cell efficiency is 23 percent. Solar flux at one AU is 1,358 W/m^2 ; at Mars, a distance of about 1.5 AU, flux decreases to 40% of its 1 AU value (604 W/m^2). Major SEP elements modeled are shown in Fig. 9. For SEP evaluations, total array power levels ranged from 20 to 45 kWe. Data shown in Fig. 20 and 21 feature a 22 kWe nominal power level, though array mass is based an additional 10% margin (24.2 kWe).

SEP ION THRUSTERS

The SEP transfer stage includes an array of 2 to 4 NASA Evolutionary Xenon Thrusters (NEXT)^{4,5} ion thrusters. NEXT thrusters, rated at 6.85 kWe, operate at 4116 sec Isp. PPU⁶s convert power from the solar array and deliver electrical power at proper voltage and current to the thruster array. The thruster elements consist of a set of thrusters, gimbals, actuators, a DICU, sun shield and support structure. A NEXT thruster is pictured in Fig. 10, and two 10 kWe Hall thrusters are shown in Fig. 11. The thruster pictured on the right, the NASA-173 v.2 design,^{7,8,9} rated at 9.95 kWe, operates at 3390 sec Isp. NEXT and NASA-173 performance is calculated using supplied Isp vs power throttle tables. An example from Ref. 10 is shown in Fig. 12.

Ion thrusters suffer from low thrust density (available thruster per unit exhaust area) because the maximum ion current density that can be sustained is limited by space-charge distortions of the applied electric field. One advantage of the Hall thruster compared to an electrostatic ion engine is that, as the plasma in the Hall effect thruster remains substantially neutral due to the presence of the electrons that constitute the Hall current, they are able to sustain higher ion current densities and hence offer greater thrust densities.

VII. Comparative Analysis

MSR CHEMICAL PROPULSION STAGES

Launch vehicle total injected mass is plotted vs propellant type and transfer stage capture mode in Fig. 16, 17 and 18. In each, all assumptions and contingencies listed in Section IV apply. Allocations for chemical stage inert, propellant, aerocapture brake, inbound payload and outbound (lander) payload masses are shown. For results shown in Fig. 16 and 17, lander release occurs previous to the Mars capture burn. In Fig. 16, Mars lander payload is fixed at 1.2 mt and total chemical stage mass is variable.

- In Fig 16, for aerobraking capture:
 - For all propulsion types, except O₂/CH₄ and H₂, injection masses are within Atlas-V 431 capabilities
 - Only F₂/N₂H₄ injected masses fall within Atlas-V 421 capabilities
 - O₂/H₂ inert mass is comparatively high due to the cryocooler requirements for storing H₂ for the Mars capture and departure burns
- In Fig 16, for aerocapture:
 - For all types, except O₂/H₂, injection masses fall within Atlas-V 431 capabilities.
 - NTO/N₂H₄ and O₂/N₂H₄ vehicle injected masses fall within Atlas-V 421 capabilities.
 - Only F₂/N₂H₄ injected masses fall within Delta-IV 4450 capabilities.
 - Aerocapture allows 0.5 mt reductions in injected mass compared to aerobraking for each of the systems.

In Fig. 17, Mars lander mass is variable and total injected mass is fixed at the Atlas-V 421 value. Lander release occurs previous to the transfer stage capture burn.

- In Fig 17, for aerobraking capture:
 - Lander masses of 1.0, 0.9, and 1.3 mt are achieved for NTO, O₂, and F₂ combinations with N₂H₄.
 - Lander payload mass of 0.4 mt is achievable for O₂/CH₄
 - O₂/H₂ does not provide any payload.
- In Fig 17, for aerocapture:
 - Lander masses of 1.5, 1.4, and 1.6 mt are achieved for NTO, O₂, and F₂ combinations with N₂H₄.
 - Lander payload mass of 1.1 mt is achievable for O₂/CH₄
 - O₂/H₂ does not achieve any payload.
 - Aerocapture allows increases in the range of 0.3 to 0.7 mt in lander mass.

In Fig. 18, Mars lander mass and injected mass are variable. Data is shown for the lander released before and after transfer stage capture into LMO. In each case shown in Fig. 18, exclusive use is made of aerocapture at Mars and NTO/N₂H₄ propulsion for Mars departure.

- In Fig 18, for lander aerocaptured with transfer stage down to LMO:
 - Lander masses of 0.7, 0.9, 1.1 and 1.4 mt are achieved for Delta-IV 4240, 4450, Atlas-V 421 and 431 capabilities. Injected masses correspond to the launchers capabilities to C3=10 km²/s².
- In Fig 18, for lander direct entry:
 - Lander masses of 0.9, 1.2, 1.460, and 1.8 mt are achieved for Delta-IV 4240, 4450, Atlas-V 421 and 431 capabilities.
 - Lander direct entry allows for lander mass increases of 0.2 to 0.45 mt as compared to combined lander-transfer stage capture.

In Fig. 19, MSR chemical stage injected mass is plotted vs aerocapture brake mass percentage. Injected mass is variable and lander mass is fixed at 1.2 mt. Data is shown for lander release previous to transfer stage capture. In each case exclusive use is made of NTO/N₂H₄ propulsion for Mars departure.

● In Fig 19

- Aerocapture brake mass percentages of 30% or greater show no advantage over aerobraking
- At an aerocapture brake percentage of 25%, injected mass is within the capability of the Atlas-V 421
- At a brake percentage of 15% and lower, injected masses are within the capability of the Delta-IV 4450
- Aerocapture captured mass percentage calculations include the mass of the aerobrake.

MSR SEP PROPULSION STAGES

MSR SEP data is shown for two example cases. The first case vehicle uses three NEXT ion thrusters and the second uses two NASA-173 Hall thrusters. In each case array power level is 22 kWe. Total thrust values at Earth and Mars distances for the ion system are 0.71 and 0.39 N respectively; for the Hall system these values are 0.73 and 0.59 N respectively. The Hall system has 50% more thrust at Mars than the ion system for roughly the same array power. SEPTOP trajectories were generated for a wide variety of launch vehicles and injection C3's; in Fig. 20 results are shown for Delta-IV 4450 injections to C3=17.2 km²/s² for the SEP NEXT ion system, and C3=10.6 km²/s² for the SEP Hall system. Earth-Mars transfer times, including Mars spiral down time, were 1.3 years for both systems. This compares to an approximately 5 month transfer time characteristic of the chemical systems injected to C3's of 10 km²/s².

Total injected mass is plotted vs transfer propulsion technology in Fig. 20. For each case Mars lander mass is fixed at 1.2 mt, lander release occurs before transfer stage capture, and launch vehicle injected mass is variable.

➤ In Fig 20

- 22 kWe SEP ion system injected mass (2.8 mt) is appreciably less than the 22 kWe SEP Hall (3.4 mt), the chemical/aerocapture (3.7 mt) and the chemical/aerobrake (4.2 mt) systems
- SEP trip times are appreciably longer
- SEP inert mass are higher, but propellant loads in the ion case are significantly less than the other cases
- SEP systems use a single propulsive technology for all maneuvers.

SEP MSR power and weight budget values are given in Fig. 21 for the 22 kWe array, 3 thruster NEXT ion system.

VIII. Conclusion

Roundtrip Mars sample return vehicles were analyzed to determine how specific technology selections influence payload delivery capability. The following statements only apply to MSR missions of the type described in this paper. Comparisons will be made to the reference NTO/N₂H₄ chemical/aerobraking vehicle. Results indicate:

1. Cryogenic O₂/H₂ and O₂/CH₄ propulsion technologies result in increased transfer stage mass
2. Advanced Fluorine engine technology provides modest decreases to transfer stage mass
3. Aerocapture technology decreases transfer stage mass significantly (if the aerocapture brake mass is 20% or less of the total captured mass)
4. Aerocapture technology, at mass fractions of 30% or above, does not provide mass reduction as compared to aerobraking options
5. SEP ion technology decreases transfer stage mass most significantly, at the cost of increased trip times

Future activities under the ISTA study are planned that will further quantify and expand upon these results.

Acknowledgments

Results presented here were generated under the NASA In-Space Technology Assessment (ISTA) contract. Special thanks go to Les Johnson, manager of NASA MSFC In-Space Propulsion, and Randy Baggett, program manager of NASA MSFC Next Generation Electric Propulsion program, for providing direction for this work. Our many thanks to Michael Cupples, Tom Percy, Gordon Woodcock, Dave Byers, Gwen Artis and Melody Hermann.

References

- ¹Sauer, C. Jr., "Optimization of Multiple Target Electric Propulsion Trajectories," AIAA 73-205, Jan. 1973.
- ²Sauer, C. Jr., "Solar Electric Propulsion Performance For Medlite And Delta Class Planetary Missions," AAS 97-726, Aug. 1999
- ³George, L.E., Kos, L.D., "Interplanetary Mission Design Handbook: Earth-Mars Mission Opportunities and Mars-Earth Return Opportunities 2009-2024," NASA/TM-1998-208533
- ⁴NASA Research Announcement Proposal Information Package Next Generation Ion Engine Technology. NASA, section A.9.2.
- ⁵Patterson, M., Thomas, M., Foster, W., Rawlin, J., Roman, V., Robert, F., Soulas, G. "Development Status of a 5/10-kW Class Ion Engine," AIAA 2001-3489, July 2001
- ⁶Piñero, L., "Design of a Modular 5-kW Power Processing Unit for the Next-Generation 40-cm Ion Engine," IEPC-01-329
- ⁷Manzella, D., Jankovsky, R., Hofer, R., "Laboratory Model 50kW Hall Thruster," AIAA-2002-3676, July 2002
- ⁸Jacobson, D., Manzella, D., "50kW Class Krypton Hall Thruster Performance," AIAA-03-4550
- ⁹Fiehler, D., Jankovsky, R., "The Influence of Current Density and Magnetic Field Topography In Optimizing the Performance, Divergence and Plasma Oscillations of High Specific Impulse Hall Thrusters," IEPC-03-142
- ¹⁰Fiehler, D., Oleson, S., "A Comparison of Electric Propulsion Systems for Mars Exploration," AIAA-2003-4574

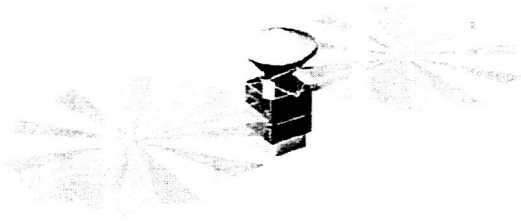


Fig. 1 SEP Configuration: lander above orbiter

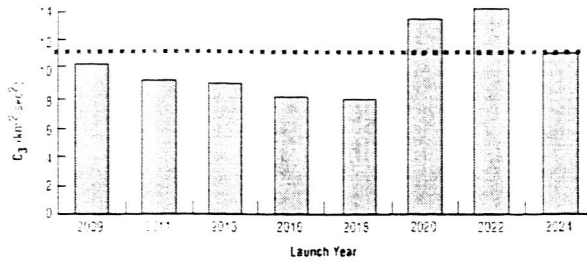


Fig. 4 Earth departure C3 vs Launch Year

Launch Vehicle	Launch Mass C3 = 0 (kg) (LV Margin 0%)	Launch Mass C3 = 10 (kg) (LV Margin 2%)
Atlas-V 431	5536	4527
Atlas-V 421	4880	3993
Delta-IV 4450	4583	3612
Delta-IV 4240	4075	3212

Fig. 2 Launch vehicle payload capabilities

	All propulsive	Propulsive/Aerobraking	Aero-capture
Outbound Leg:			
- Trans-Mars Injection	0	0	0
- Outbound midcourse correction	30	30	30
Mars Arrival: ($V_{hp} = 3.0$)			
-MOI propulsive capture	2,261	1,097	0
-Corrective maneuvers	0	101	135
Rendezvous: (with Ascent stage)	100	100	100
Mars Departure: ($V_{hp} = 3.1$)			
- Trans Earth Injection	2,315	2,315	2,315
Inbound Leg:			
- Inbound midcourse correction	30	30	30
- Earth Divert maneuver	40	40	40
G-Losses: - 2% of total	96	74	53
Total:	4,872	3,787	2,703
Percentage	100 %	78 %	55 %

Fig. 5 Chemical transfer stage dV sets

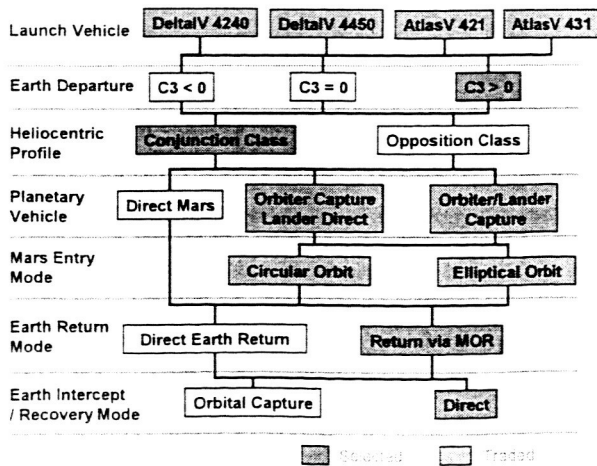


Fig. 3 Trajectory trade options

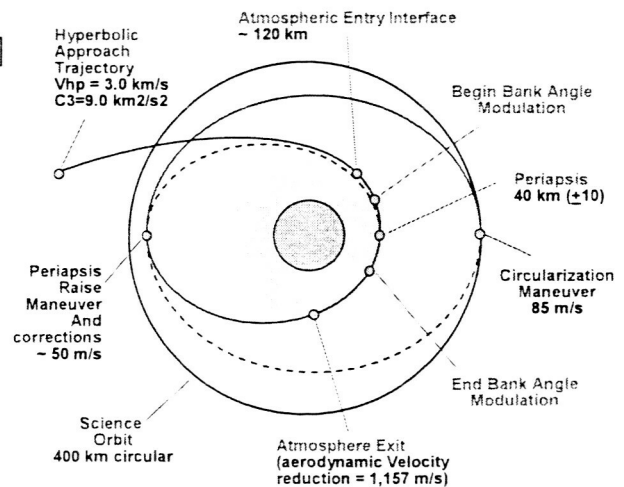


Fig. 6 Mars aerocapture parameters

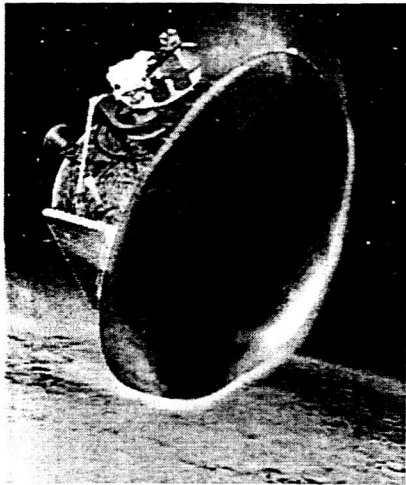


Fig. 7 Mars aerocapture



Fig. 10 NEXT Ion

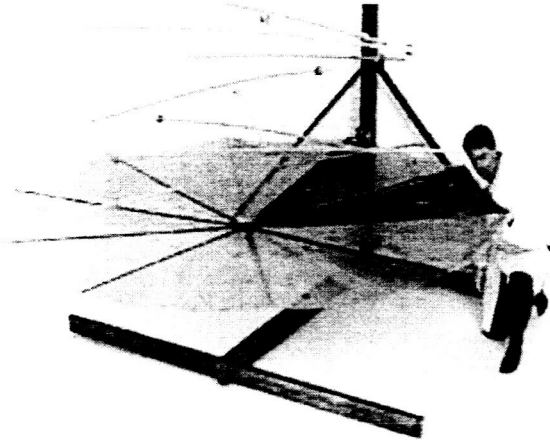
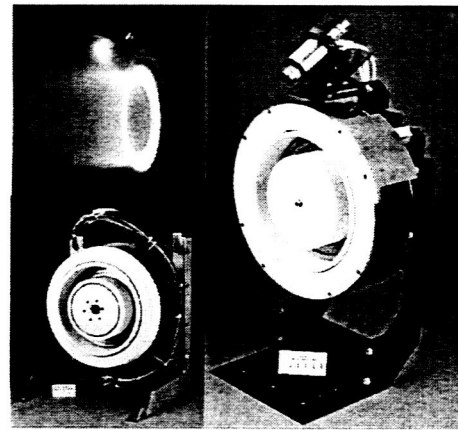


Fig. 8 AEC-Able SolarFlex



10 kW T-220 Pratt & Whitney 10 kW NASA-173 v2 GRC

Fig. 11 10 kWe Hall thrusters

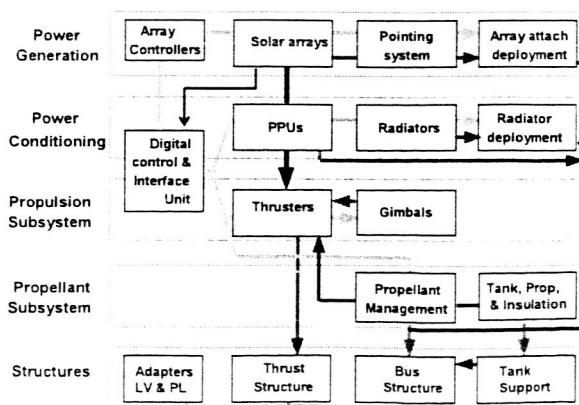


Fig. 9 Major SEP elements modeling

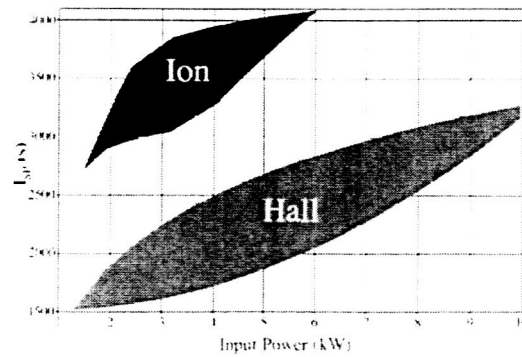


Fig. 12 Example Isp vs Input

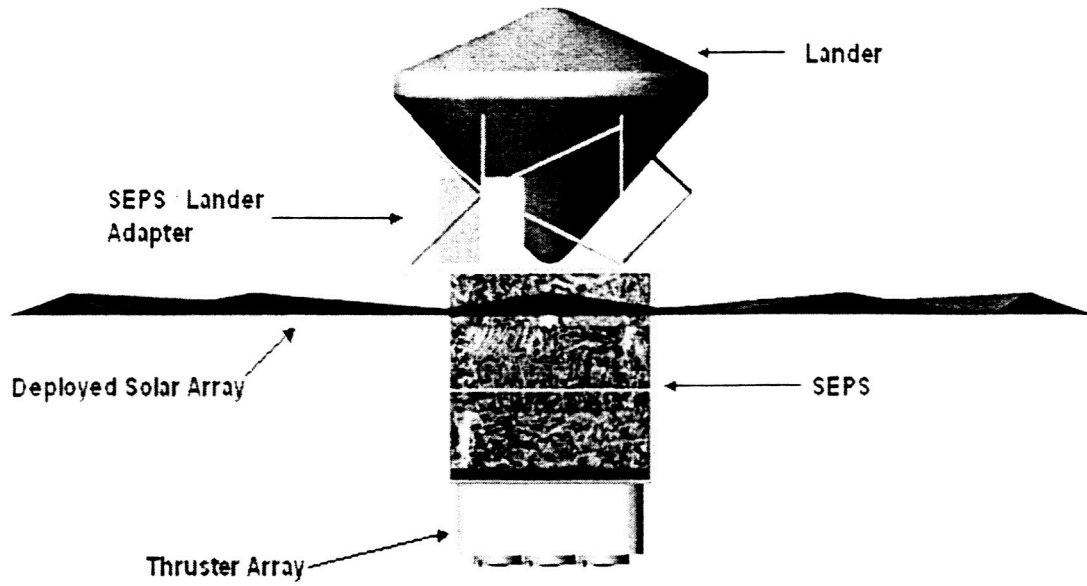


Fig. 13 SEP configuration: side view

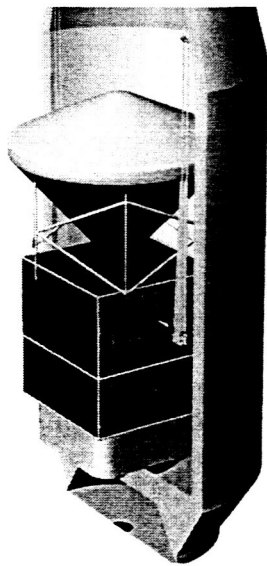


Fig. 14 Stowed configuration

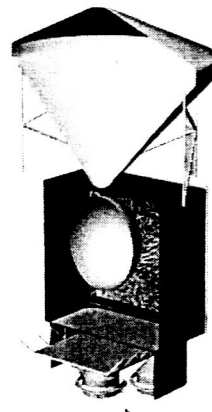


Fig. 15 Cutaway showing Xenon tank

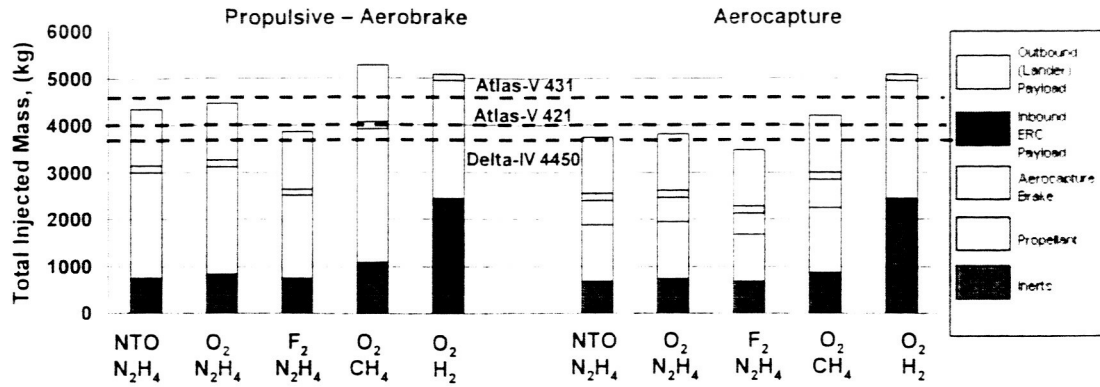


Fig. 16 Total injected mass vs propellant type for 1200 kg outbound payload

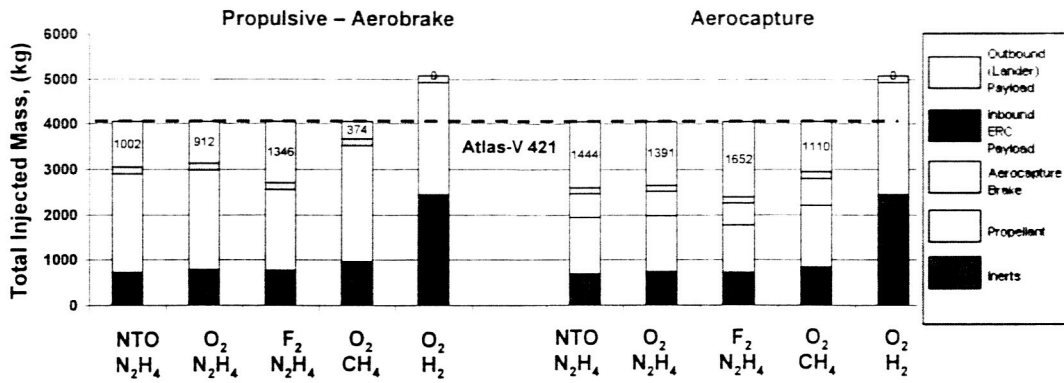


Fig. 17 Outbound chemical payload and inject mass vs propellant type for Atlas-V 421

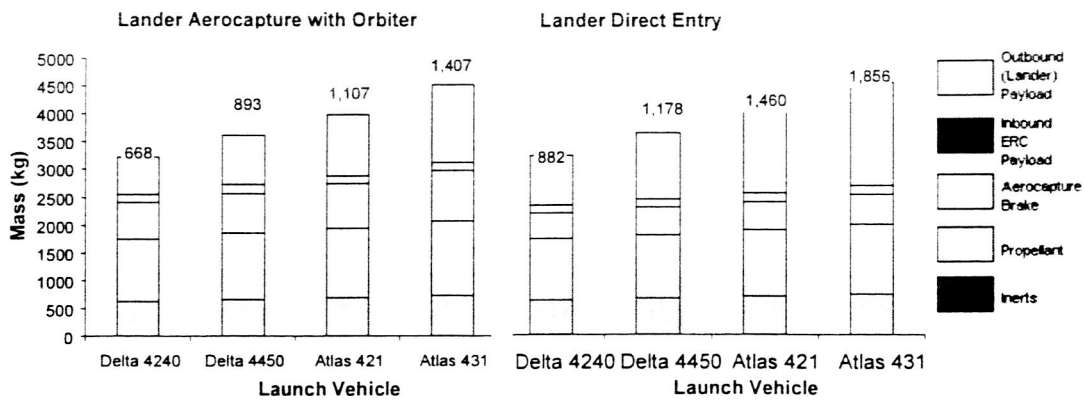


Fig. 18 Total injected mass and chemical payload vs launch vehicle and entry mode

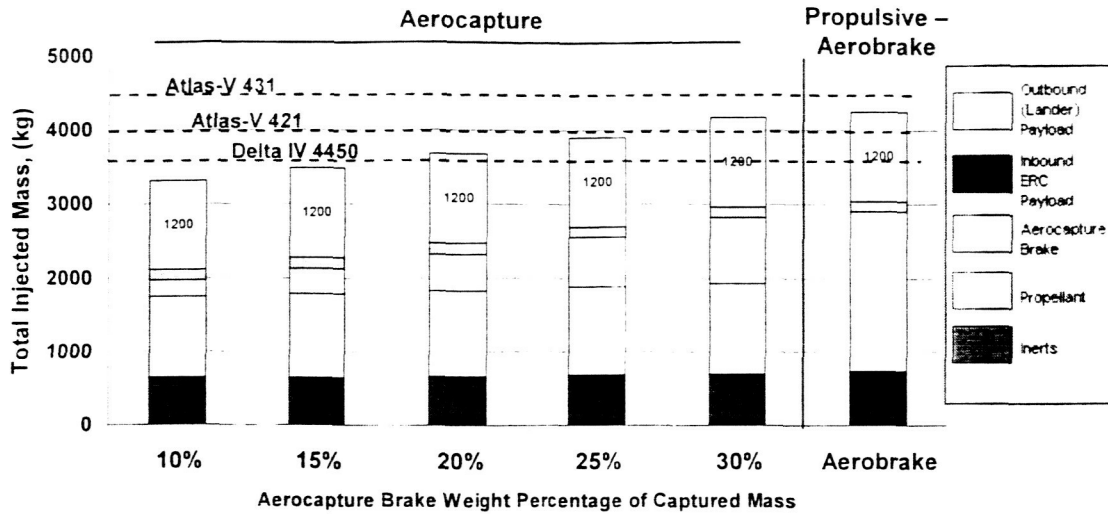


Fig. 19 Total injected mass vs aerocapture brake percentage of captured mass

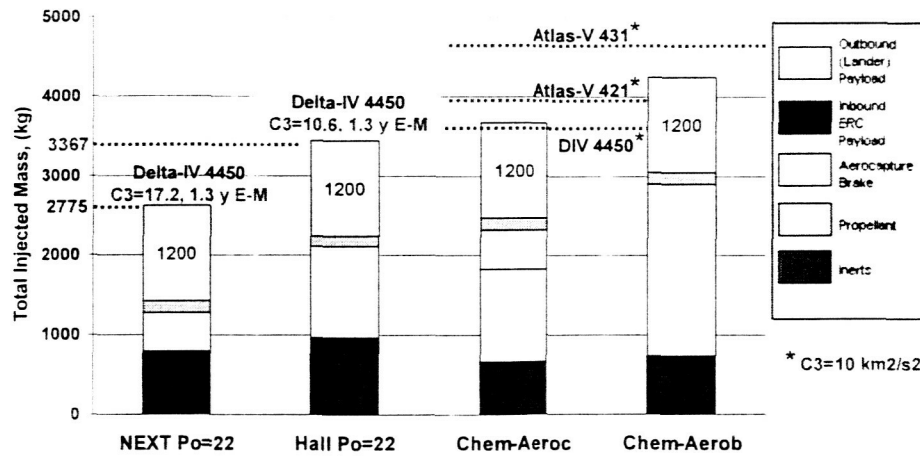


Fig. 20 Injected mass vs propulsion technology

	Earth	Mars	Unit	Margin	Total
Power Budget:				kg	kg
AU - array -	1.00	1.50		103	134
Sunlight Intensity	1.358	604	W/m ²	30	40
Array Area w margin and packing Eff	10% 96.8	96.8	m ²	199	209
Array Area Required	70.4	70.4	m ²	55	72
Array Power for Costing	cell eff 24.2		kWe	23	31
Array Power	23.0% 22.0	9.78	kWe	90	117
- Po into IPS -				15	20
Housekeeping Power	0.25	0.25	kWe	32	42
Power Feathered	ax allowed 0.10	0.0	kWe	37	49
Act max power IPS	22.00	9.53	kWe	9	12
into cable to ppu	99.5%	9.48		32	42
- into PPU and Thrusters -				ACS	
Act max into PPU's	95.4%	9.48	kWe	Other	
into cable to thruster	100.0%	9.48		Telecom, C&DH	42
Act max Po Thrusters	69.8%	8.97	kWe	GN&C	26
Thrust total	0.71	0.31	N	Other	23
				Rendezvous Instr Suite	52
				Reserves	51
				Propellant Inbound	152
				Rendezvous	3
				Outbound	354
				Payload Outbound	1,165
				Inbound	183
				Launch Mass	2,775

Fig. 21 SEP MSR power and weight budget (22 kWe)